Bulletin of Geography. Physical Geography Series, No. 28 (2025): 65–80
http://doi.org/10.12775/bgeo-2025-0005

Satellite and gauge-based precipitation dataset assessment in Thua Thien Hue (Vietnam)

Nguyen Thai Son[1], Nguyen Tien Thanh[2a]*

[1]Vietnam Academy of Science and Technology, Institute of Geography, Cau Giay, Ha Noi, Vietnam

[2]Thuyloi University, 175 Tay Son, Dong Da, Ha Noi, Vietnam

*E-mail: thanhnt@tlu.edu.vn

[a]https://orcid.org/0000-0002-1995-2568

Abstract. Thua Thien Hue, a central province of Vietnam, has a monsoon tropical climate and complex interaction of weather patterns and topography and, particularly, very sparse of in-situ precipitation observations to model the hydrological characteristics for flood monitoring. So, this study evaluates the performance of four satellite-based precipitation datasets (CHIRPS, GSMaP, GPM and MSWEP) against gauge-based precipitation observations in Thua Thien Hue from 2020 to 2023. Tthe accuracy of each dataset is evaluated based on Taylor diagrams, Mean Absolute Error (MAE), Root Mean Square Error (RMSE), correlation coefficient (R), Critical Success Index (CSI), Probability Of Detection (POD) and False Alarm Ratio (FAR). Results show that MSWEP exhibits the highest correlation (R=0.58), lowest RMSE (23 mm/day), and best agreement with observed rainfall, making it the most reliable dataset. GSMaP follows, with strong correlation (R=0.63) but higher RMSE, indicating good temporal alignment but greater variability in extreme events. In contrast, CHIRPS and GPM have weaker correlations (R<0.40) and higher RMSE (>50 mm/day), leading to frequent underestimation of precipitation. The findings highlight systematic biases in satellite precipitation estimates and emphasize the need for regional calibration and bias correction. The study suggests that MSWEP is a useful source of data and should be prioritized for hydrological modeling in the region.

Key words:
GSMaP,
GPM,
MSWEP,
CHIRPS,
Taylor diagram,
continuous statistical metric,
Thua Thien Hue

Introduction

Currently, there are many grid precipitation products developed using remote-sensing data on a global scale, such as the Global Satellite Mapping of Precipitation (GSMaP) (Ushio et al. 2004), Global Precipitation Measurement (GPM) (Kidd and Huffman 2011), Tropical Rainfall Measuring Mission (TRMM) (Simpson et al. 1988), Climate Hazards group InfraRed Precipitation with Stations (CHIRPS) (Funk et al. 2015), Climate Prediction Center (CPC) MORPHing Version 1.0 (CMORPH_V1.0) (Joyce et al. 2004), Precipitation Estimation from Remotely Sensed Information using Artificial Neural Network (PERSIANN) (Ashouri et al. 2015), and Multi-Source Weighted-Ensemble Precipitation (MSWEP) (Beck et al. 2019). Each of these grid precipitation products is created from different types of sensors, such as passive microwave (PMW) or near-infrared (NIR), and employs various algorithms to compute data at different spatial and temporal resolutions. Therefore, the quality of these satellite grid precipitation products is not uniform and varies in accuracy when applied to different regions. Burton et al. (2018) indicated that CHIRPS performs best in South America and the tropical regions of Africa, while CHIRPS and TRMM have similar quality in Southeast Asia.

Zhou et al. (2020) showed that GSMaP yields very good results in southern China. Luo et al. (2024) analyzed sixteen products of precipitation including observation-based, satellite-based, reanalysis data, multi-source merged precipitation products, and products from numerical weather models. The results showed the best product of multi-source merged precipitation and an underestimation of the model-based precipitation products compared to the observation for the mountain torrents. Ji et al. (2022) showed the potential precipitation products for modeling the hydrological characteristics for Yarlung Zangbo River Basin. The products include TRMM3B42, PERSIANN-CDR, Global Precipitation Measurement (GPM), CMORPH and GSMaP. The results indicate that GPM and CMORPH yield satisfactory results, whereas TRMM outperformed GPM in modeling runoff with smaller relative error. Pang et al. (2023) investigated five products of precipitation in China and showed that a precipitation fusion product is better than any single-source precipitation product. A similar performance is found for satellite-based data of IMERG, GSMAP and reanalysis. Lyu et al. (2024) evaluated twelve global precipitation datasets with a consistent tendency to overestimate and underestimate, respectively, lower and higher precipitation rates on the Tibetan Plateau. In Vietnam, Hai and Tuan (2018) pointed out that CHIRPS and GPM precipitation demonstrate a good representation of rainfall distribution in the lowland and coastal areas of the Ca River basin. Thanh (2019) also evaluated the quality of precipitation from various sources for the Vu Gia – Thu Bon River basin and indicated that TRMM provides the best results, whereas CMORPH performs well at low rainfall thresholds. There is every indication that no single satellite product can achieve optimal accuracy under all conditions; however, it is important to highlight the strengths of each product in relation to local characteristics. It is especially noted that in-situ precipitation observations in Thua Thien Hue are limited and very sparse.

The Vietnamese climate has both tropical and monsoon characteristics due to the country being completely covered by the domain of intertropical zone and monsoon. According to statistical yearbooks of Vietnam, during 1972–2021, 156 tropical depressions and 479 storms were active in the East Sea, of which 180 storms had the highest intensity of level 8–9, 132 storms were level 10–11, 164 were of level 12–15, and three were level 16 or higher. Of 635 storms and tropical depressions, 236 directly affected the mainland of Vietnam (MONRE 2022). Consequently, the climate regime from region to region is unevenly distributed in space and time. Combined with the topographic conditions of mountainous and hilly regions, a high frequency of extreme events is recorded in the whole country. Thua Thien Hue Province is one of the most disaster-prone areas in Vietnam, being characterized by a high concentration of storms, with the region from Thanh Hoa to Thua Thien Hue accounting for 57.3% of all storms in the country. This province also experiences some of the highest rainfall levels in Vietnam, which, combined with frequent flooding, leads to significant damage to property and loss of life. Historically, Thua Thien Hue has faced numerous flooding events with considerable frequency and intensity. Typically, between 1802 and 1884, the province experienced 32 floods, including a notable event in 1811 when the Imperial City was inundated by 3.6 meters of water. From 1885 to 1945, there were six major floods, and from 1946 to 1975, 39 storms occurred, including a historic flood in 1953. The period from 1976 to 2006 saw 30 floods, with 11 classified as major, including a significant flood in 1999 that was unprecedented in a century. This flood resulted from excessive rainfall, with total precipitation reaching 2,288 mm over six days, and a peak daily rainfall of 1,422 mm. The consequences were devastating, with 372 fatalities, nearly 600 people missing, and approximately 570,000 homes inundated, leading to an estimated economic loss of around VND 1,800 billion. The province continued to face severe flooding challenges in the years that followed, particularly in 2009 and 2020. The October 2020 floods were particularly catastrophic, resulting in at least 45 deaths and affecting 85,000 homes, with total economic losses exceeding VND 2,000 billion (PCTTHP 2005; PCTTHP 2020).

Daily or sub-daily precipitation data is extremely essential for analyzing the impacts of meteorological forcings on various agricultural, natural resource and hydrological models in particular; however, accurately quantifying it at daily and sub-daily temporal scales poses challenges for meteorologists and hydrologists. This issue is particularly pronounced in tropical regions, where precipitation is strongly disturbed in space and time (Saikranthi et al. 2013). Parallel to the effects of topography, consequently, precipitation can fluctuate rapidly due to convection processes. Meanwhile, presently, the gridded precipitation products have not been thoroughly evaluated for Thua Thien Hue Province, located in central Vietnam. So, it is especially important to interpret the quality of satellite-based precipitation dataset assessment in Thua Thien Hue. Accordingly, the study aims at evaluating the quality of satellite-based precipitation against gauged-based precipitation with available daily and sub-daily data during 2020–2023.

Materials and methods

Study area

Thua Thien Hue's climate and topography create a highly dynamic and risk-prone environment, where the interaction between atmospheric and geomorphological factors drives extreme hydrological events. The province experiences a tropical monsoon climate, with distinct wet and dry seasons that influence water availability, flood risk and land use. During the rainy season (September–December), intense and prolonged rainfall, exacerbated by orographic effects from the Truong Son Mountains, leads to rapid runoff and flash floods in upstream areas. This runoff accumulates in the low-lying coastal plains, where slow drainage and tidal influence prolong flood durations, particularly in Hue City and the Tam Giang – Cau Hai Lagoon system. Meanwhile, in the dry season (January–August), the dominance of hot, dry westerly winds reduces moisture levels, increasing drought susceptibility and affecting agricultural productivity.

Topographically, the province transitions from steep, forested mountains in the west to narrow river valleys and coastal plains in the east. This gradient accelerates hydrological response times, meaning rainfall in the highlands quickly translates into downstream flooding. The Tam Giang Lagoon acts as a temporary water storage system but can become a flood amplifier when excessive inflows exceed its capacity. Additionally, the coastline is highly exposed to typhoon-induced storm surges, which, when combined with fluvial flooding, intensify disaster impacts. The convergence of high rainfall variability, steep terrain and complex hydrodynamics makes Thua Thien Hue particularly vulnerable to flooding, landslides and saltwater intrusion.

Data sources and characteristics

GSMaP

The Global Satellite Mapping of Precipitation (GSMaP) is a satellite-based precipitation dataset that provides high-resolution, near-real-time rainfall estimates worldwide. Derived from multiple satellite observations, including the Global Precipitation Measurement (GPM) mission, GSMaP offers spatial resolutions of 0.1° (~10 km) and temporal resolutions ranging from hourly to monthly. It integrates data from various sensors using advanced algorithms to enhance accuracy, making it particularly valuable for regions lacking ground-based measurements. GSMaP supports applications in weather forecasting, hydrology, disaster management and climate research. The dataset is available in formats such as netCDF and GeoTIFF and undergoes rigorous validation against ground-based observations to ensure reliability.

CHIRPS

Climate Hazards InfraRed Precipitation with Station Data (CHIRPS) is a high-resolution quasi-global rainfall dataset covering latitudes from 50°S to 50°N from 1981 to the present. It integrates satellite-derived precipitation estimates with in-situ rain gauge data to provide gridded rainfall records at a 0.05° spatial resolution. CHIRPS is widely used for climate research, drought monitoring, agricultural assessments and hydrological studies. The dataset undergoes systematic bias corrections and is accessible in multiple formats for various analytical applications. Its reliability and long-term consistency make it a key resource for understanding climate variability and informing policy decisions related to water resources and disaster preparedness.

MSWEP

The Multi-Source Weighted-Ensemble Precipitation (MSWEP) dataset provides global, high-resolution precipitation estimates with a 3-hour temporal resolution and 0.1° spatial resolution, spanning 1979 to the present. It combines data from multiple sources, including ground-based rain gauges (GPCC, CPC Unified), satellite-based products (CMORPH, GSMaP, TMPA) and reanalysis datasets (ERA-Interim, JRA-55). To improve accuracy, MSWEP employs bias-correction techniques, including a Budyko-type equation that utilizes streamflow data from approximately 14,000 catchments worldwide. The dataset is particularly useful for hydrological applications, including streamflow simulation, soil moisture modeling and evaporation estimation. MSWEP has demonstrated superior performance in regions with sparse rain gauge networks, making it a valuable tool for hydrology and climate science.

IMERG-GPM

The Integrated Multi-satellite Retrievals for GPM (IMERG) algorithm generates high-resolution global precipitation estimates by merging data from the Global Precipitation Measurement (GPM) satellite constellation. Launched in 2014, GPM enhances precipitation monitoring and forecasting by integrating microwave and infrared satellite observations with ground-based rain gauge measurements. IMERG employs intercalibration techniques to improve data consistency, making it a crucial tool for hydrological modeling, climate studies and disaster risk management. The near-real-time availability of IMERG data facilitates rapid response to extreme weather events.

Rain gauge data

Hourly precipitation data were collected from 20 rain gauge stations across Thua Thien Hue Province between 2020 and 2023. These stations are Nham_Aluoi (0), HoHoaMy (1), HoToSon (2), Adot Aluoi (3), HuongNguyen Aluoi (4), GiangHai (5), Dap TĐTN (6), LocTien (7), HoMyXuyen (8), TTSIa (9), QuanTuongDai (10), TTALuoi (11), TTPhuDa (12), HoALa (13), TaLuong (14), HongVan (15), HoChuaNuocTruoi (16), HCKheNgan (17), HCThuyYen (18), TTKheTre (19). The spatial distribution and coordinates of these stations are illustrated in Figure 1.

Method

To assess the performance of the selected precipitation estimates, this study employs continuous statistical metrics. The Mean Absolute Error (MAE) quantifies the average error magnitude, with an optimal value of 0, as defined in Equation 1. The Root Mean Square Error (RMSE), presented in Equation 2, assigns greater weight to larger errors compared to MAE, providing a measure of the overall error magnitude. The correlation coefficient (r), calculated using Equation 3, evaluates the linear relationship between the estimated and observed precipitation values, indicating the degree of agreement between the datasets.

$$MAE = \frac{1}{N}\sum_{i=1}^{N}|S_i - O_i| \tag{1}$$

$$RMSE = \sqrt{\frac{1}{N}\sum_{i=1}^{N}(S_i - O_i)^2} \tag{2}$$

$$r = \frac{\sum_1^N (S_i - \bar{S})(O_i - \bar{O})}{\sqrt{\sum_{i=1}^N (S_i - \bar{S})^2}\sqrt{\sum_{i=1}^N (O_i - \bar{O})^2}} \tag{3}$$

where S_i is the value of considered precipitation estimates for the *i*th daily event, O_i is the value of measured precipitation for the *i*th daily event, N is the number of precipitation events, $\overline{S_i}$ is the average value of considered precipitation product for N daily events over each grid box, and $\overline{S_i}$ is the average value of measured precipitation for N daily events over each grid box.

Furthermore, this study utilizes several categorical metrics to evaluate the rain-detection capabilities of the selected precipitation estimates. The Threat Score (Critical Success Index, CSI) quantifies the proportion of observed precipitation events that are accurately detected by the precipitation products. The Probability Of Detection (POD) represents

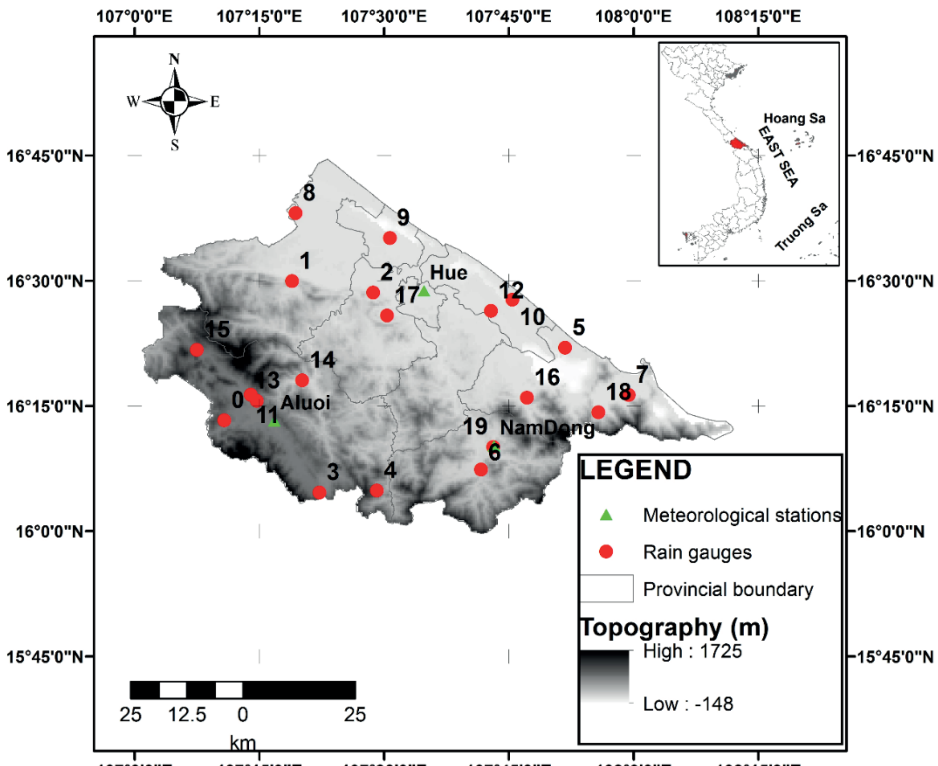

Fig. 1. Meteorological stations and rain gauges in Thua Thien Hue
Note: Nham_Aluoi (0), HoHoaMy (1), HoToSon (2), Adot Aluoi (3), HuongNguyen Aluoi (4), GiangHai (5), Dap TĐTN(6), LocTien (7), HoMyXuyen (8), TTSIa (9), QuanTuongDai (10), TTALuoi (11), TTPhuDa (12), HoALa (13), TaLuong (14), HongVan (15), HoChuaNuocTruoi (16), HCKheNgan (17), HCThuyYen (18), TTKheTre (19)

the ratio of correctly identified precipitation events to the total number of observed occurrences. The False Alarm Ratio (FAR) measures the proportion of instances where precipitation is recorded by the dataset but not observed in ground measurements. The Probability Of False Detection (POFD) calculates the ratio of false alarms to the total number of non-precipitation events in the observed dataset. These indices are formally defined in Equations 4 to 7.

$$CSI = \frac{hits}{hits + misses + false\ alarms} \quad (4)$$

$$POD = \frac{hits}{hits + misses} \quad (5)$$

$$FAR = \frac{misses}{hits + misses} \quad (6)$$

$$POFD = \frac{false\ alarms}{correct\ negatives + flase\ alarms} \quad (7)$$

Where *hits* represent the number of times that observed rain is correctly detected, *misses* indicate the number of times that observed rain is not detected, *correct negatives* indicate the number of times that rain is not detected but not observed, and *false alarms* are the number of times that rain is detected but not observed. It is noted that a threshold of 0.6 mm/day is used to distinguish between rain and no rain.

Results and discussion

Temporal Performance Evaluation

It is worth noting that, to provide uniformity of resolution, the gridded precipitation such as provided by GSMaP, CHIRPS, MSWEP and IMERG-GPM is interpolated using the bilinear interpolation algorithm to measured points (Press et al. 1992). All data are freely downloaded from the links of https://sharaku.eorc.jaxa.jp/GSMaP/ for GSMaP, https://www.chc.ucsb.edu/data/chirps for CHIRPS, https://www.gloh2o.org/mswep/ for MSWEP and https://gpm.nasa.gov/data/imerg for IMERG-GPM. All pre-processing is implemented in Linux operation using the bash scripts. The data from rain gauges is interpolated using Inverse distance weighted method in ArcGIS in spatial.

Figure 2 shows the Taylor diagrams for Thua Thien Hue in 2020 (a), 2021 (b), 2022 (c) and 2023 (d). Notably, from the datasets of the 20 rain gauges, median values are used for plotting Taylor diagrams in this study. It is observed that GSMaP consistently shows the highest correlation with OBS, at approximately 0.9 in 2020 and 2021, followed by MSWEP and GPM; by contrast CHIRPS exhibits the lowest agreement in 2020 and GSMAP in 2021. In terms of MAE, CHIRPS and GSMaP generally tend to have higher errors, whereas MSWEP and GPM perform better. Furthermore, in terms of RMSE, GSMaP and MSWEP are closer to OBS, suggesting better consistency in 2020, 2022 and 2023. In 2021, as shown in Figure 2b, the best product is MSWEP, with an RMSE value of 23 mm per day. Overall, GSMaP and MSWEP provide the most reliable estimates, whereas CHIRPS importantly requires bias correction for improved accuracy.

Figure 3 illustrates the Critical Success Index (CSI) values for various rainfall products. The results indicate that the GSMap product has the best performance, followed by MSWEP. However,

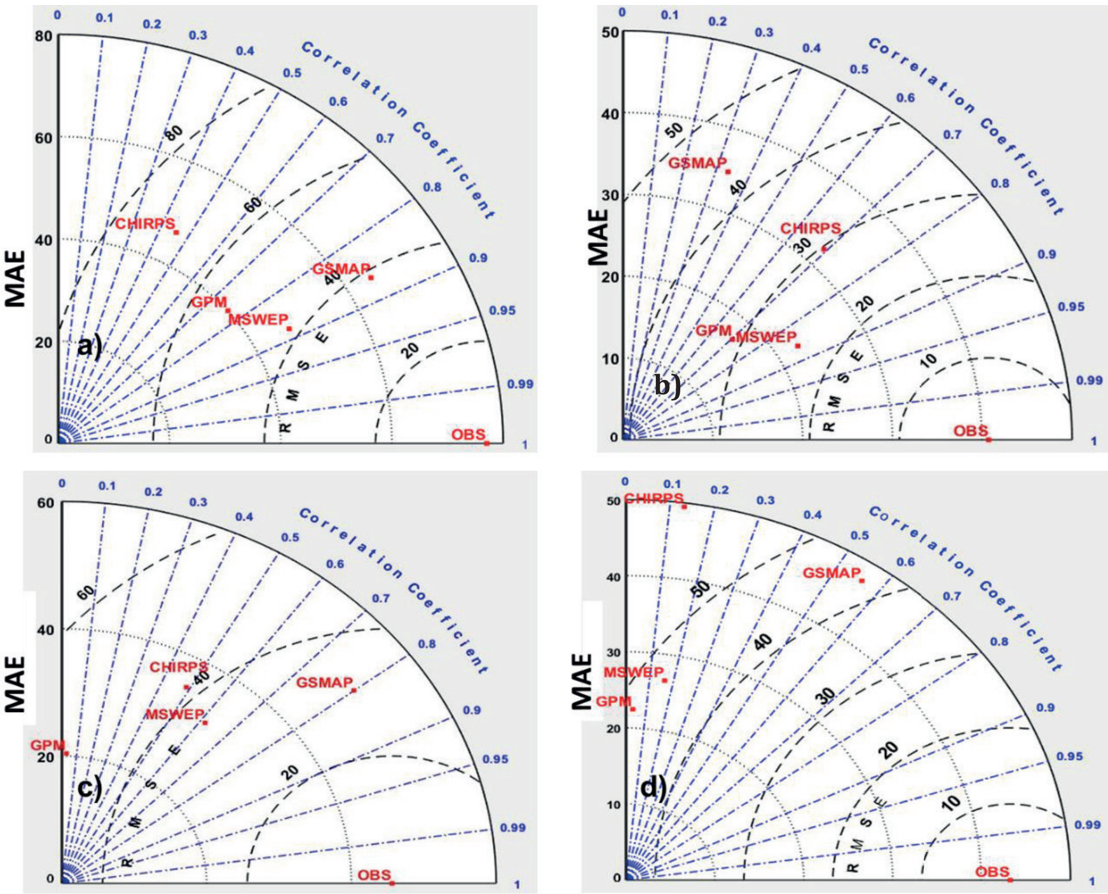

Fig. 2. Taylor diagrams in 2020 (a), 2021 (b), 2022 (c) and 2023 (d)

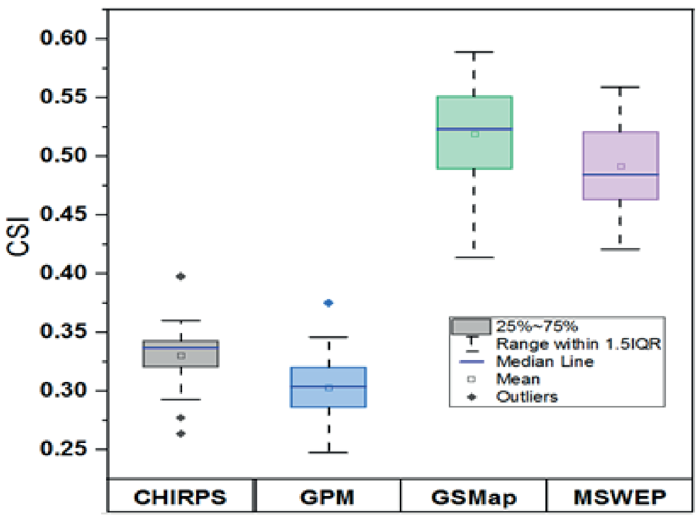

Fig. 3. CSI values for different precipitation

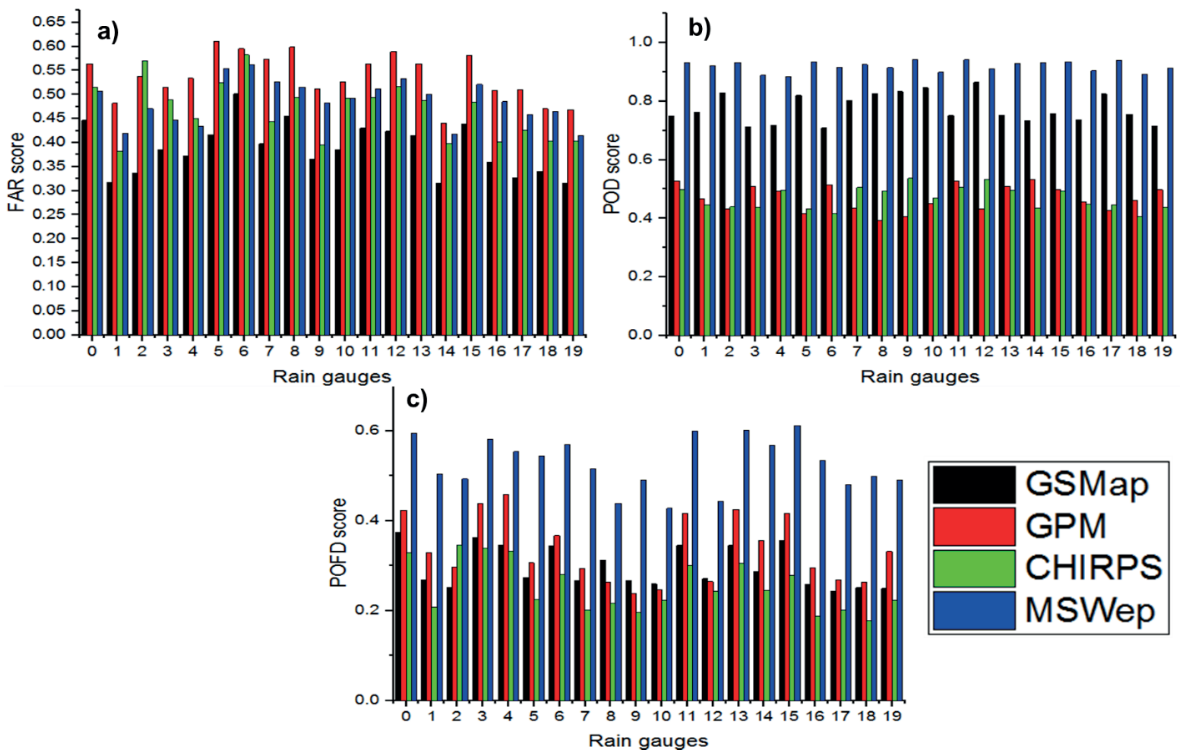

Fig. 4. FAR (a), POD (b) and POFD (c) scores for different precipitation during 2020–2023

the differences between these rainfall products are trivial, with CSI values hovering around 0.5. The CSI values around 0.5 suggest that, there are nevertheless instances of missed events and false alarms. Unlike the Probability of Detection (POD) and False Alarm Ratio (FAR), the CSI accounts for both false alarms and missed events, making it a more balanced measure. However, it is important to note that the CSI is highly sensitive to rare events and often yields lower values. Historically, Thua Thien Hue experienced significant meteorological and hydrological anomalies during 2020–2023, with tropical cyclones continuously making landfall. Therefore, the CSI values around 0.5 also suggest

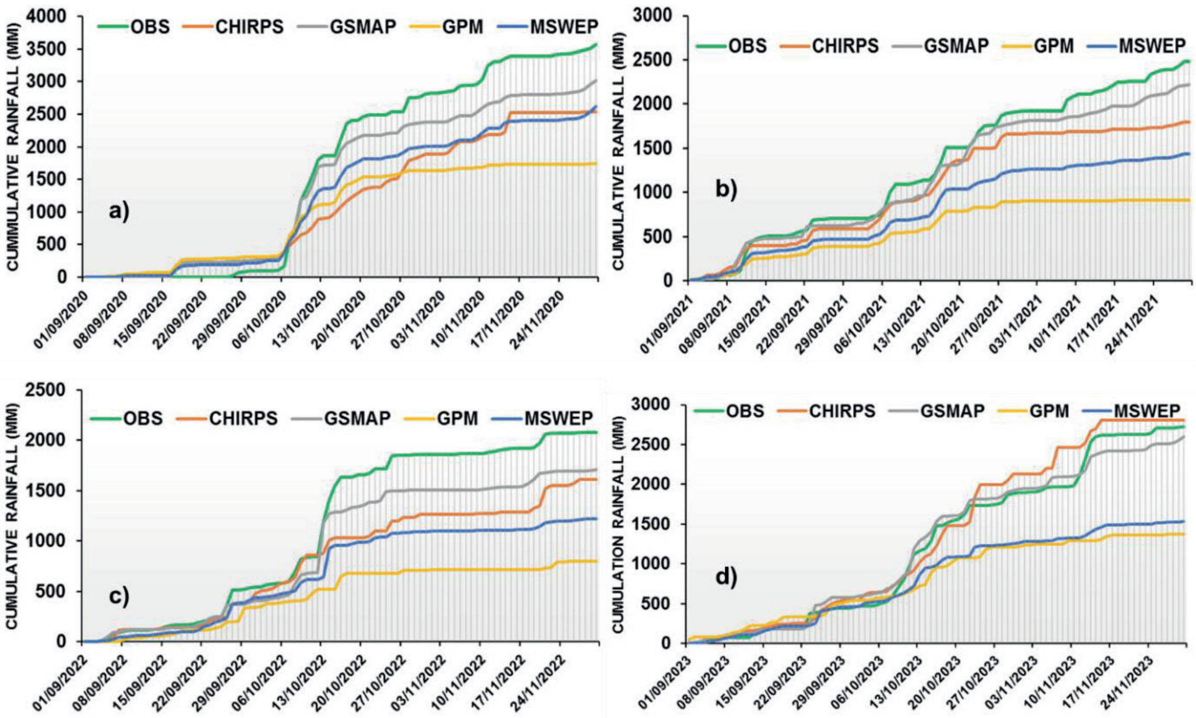

Fig. 5. Cumulative rainfall from satellite and gauge-based datasets in 2020 (a), 2021 (b), 2022 (c) and 2023 (d)

that satellite and radar rainfall products are quite effective in capturing rainfall events in general. In contrast, the CHIRPS and GPM products exhibit the lowest CSI values, indicating poorer performance.

Figure 4a shows that GSMaP and CHIRPS perform better in terms of false alarms, whereas GPM is less reliable due to frequent overestimations. As Figure 4b shows, MSWEP performs best in terms of rainfall detection, whereas CHIRPS and GPM struggle to capture all observed rainfall events (Fig. 4b). Importantly, CHIRPS, GPM and GSMaP have the lowest false detection rates, making them more reliable in differentiating between actual and no-rain conditions. Figure 4c illustrates that CHIPRS is the best product to detect false alarms.

It is specially noted that FAR reflects the reliability of rainfall predictions by considering only the cases that rain is forecasted, whereas POFD indicates how well a dataset avoids false alarms in dry conditions by considering no-rain cases. In other words, FAR provides insight into the reliability of rainfall predictions, indicating the proportion of false alarms among all predicted rainfall events. In contrast, POFD measures the frequency with which a dataset incorrectly forecasts rainfall during dry conditions. The evaluation of four precipitation datasets across multiple rain gauges reveals clear performance differences. MSWEP consistently outperforms other datasets in all three metrics, suggesting higher detection accuracy and reliability. GPM follows with moderate performance, while CHIRPS and GSMaP generally exhibit lower scores. The score of POD is highest for MSWEP, indicating its superior capability in capturing precipitation events. The remaining scores suggest that GSMaP and CHIRPS struggle with overestimations and underestimations. Overall, MSWEP is the most robust dataset, whereas CHIRPS and GSMaP show limitations in accuracy and consistency.

In terms of hydrological applications, it is important to further explain the variability of cumulative rainfall during the flood season. Accordingly, a cumulative rainfall comparison was performed between observed (OBS) and four satellite-based datasets including CHIRPS, GSMaP, GPM and MSWEP (Fig. 5). Figure 5 shows significant variability in accuracy with the green color for OBS. The results illustrate that MSWEP and GSMaP exhibit the best agreement with OBS, though they tend to slightly underestimate extreme rainfall. CHIRPS and GPM show the weakest performance, often significantly underestimating or, in some cases, overestimating precipitation. Over multiple years, GSMaP demonstrates the closest alignment with OBS, whereas CHIRPS shows inconsistencies. These findings emphasize the need for regional calibration and bias correction to improve the accuracy of satellite-based precipitation estimates for hydrological applications.

Spatial distribution and bias analysis

As the first step of visual verification, a comparison between measured precipitation and considered precipitation estimates is implemented at various spatio-temporal distributions. Figure 6 shows the spatial distribution of precipitation datasets during Sep–Nov of 2020 from different datasets. As Figure 6 shows, MSWEP relatively closely matches with observed rainfall patterns, particularly in the northern regions where the highest precipitation is recorded. However, some local discrepancies remain, with certain areas showing over- or underestimation (Fig. 6a). Importantly, GSMaP shows a better representation than CHIRPS and GPM, with higher rainfall values in the northern and central regions. However, it still underestimates extreme precipitation compared to observations, though its spatial patterns align more closely with MSWEP (Fig. 6d). CHIRPS could capture the general spatial trend but underestimates precipitation across most of the region. The spatial variation is less pronounced, suggesting that CHIRPS struggles to detect localized heavy rainfall events accurately (Fig. 6b). Generally, MSWEP and GSMaP demonstrate better agreement with observations, making them more reliable datasets for regional precipitation estimation. CHIRPS and GPM significantly underestimate rainfall, limiting their effectiveness in capturing extreme events.

Similarly, as Figure 7 shows, MSWEP demonstrates a reasonably good alignment with

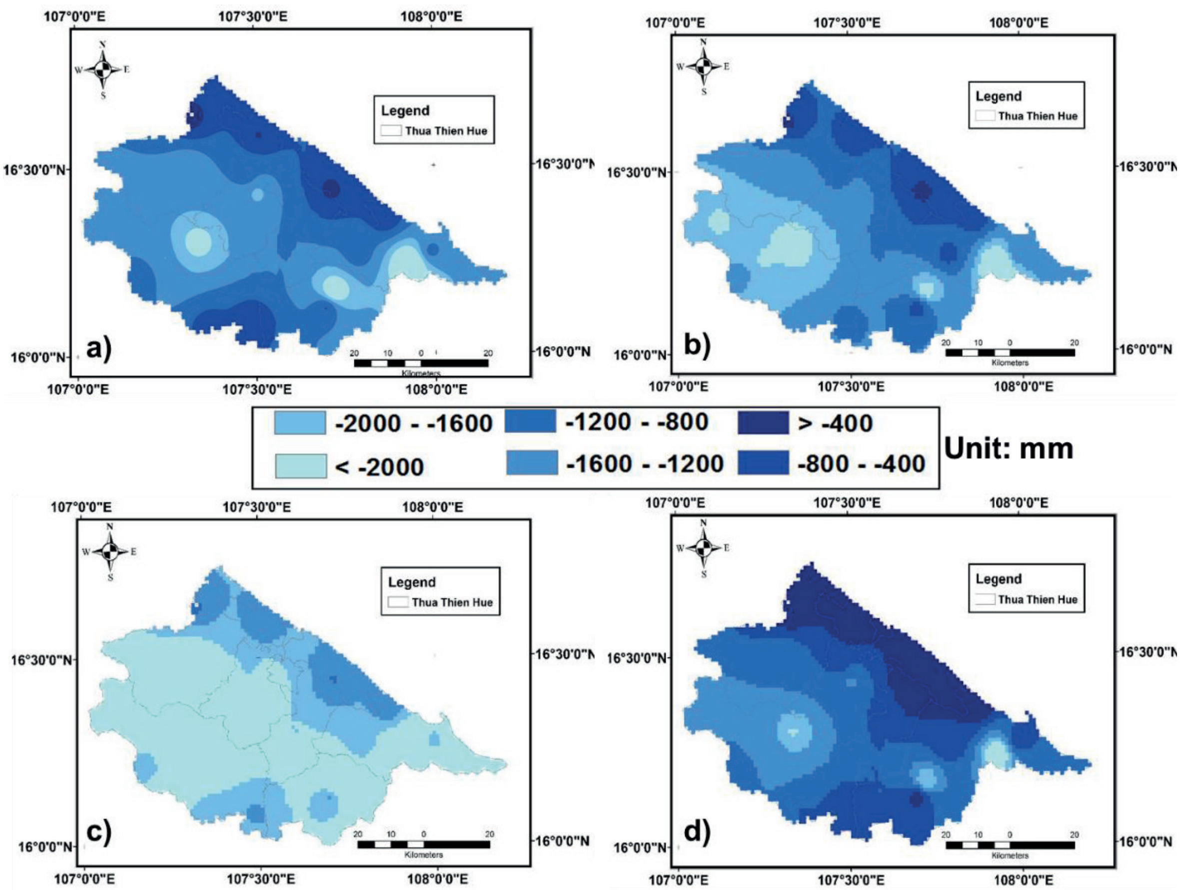

Fig. 6. Spatial distribution of precipitation datasets against observation for MSWEP (a), CHIRPS (b), GPM (c) and GSMAP (d) during Sep–Nov of 2020

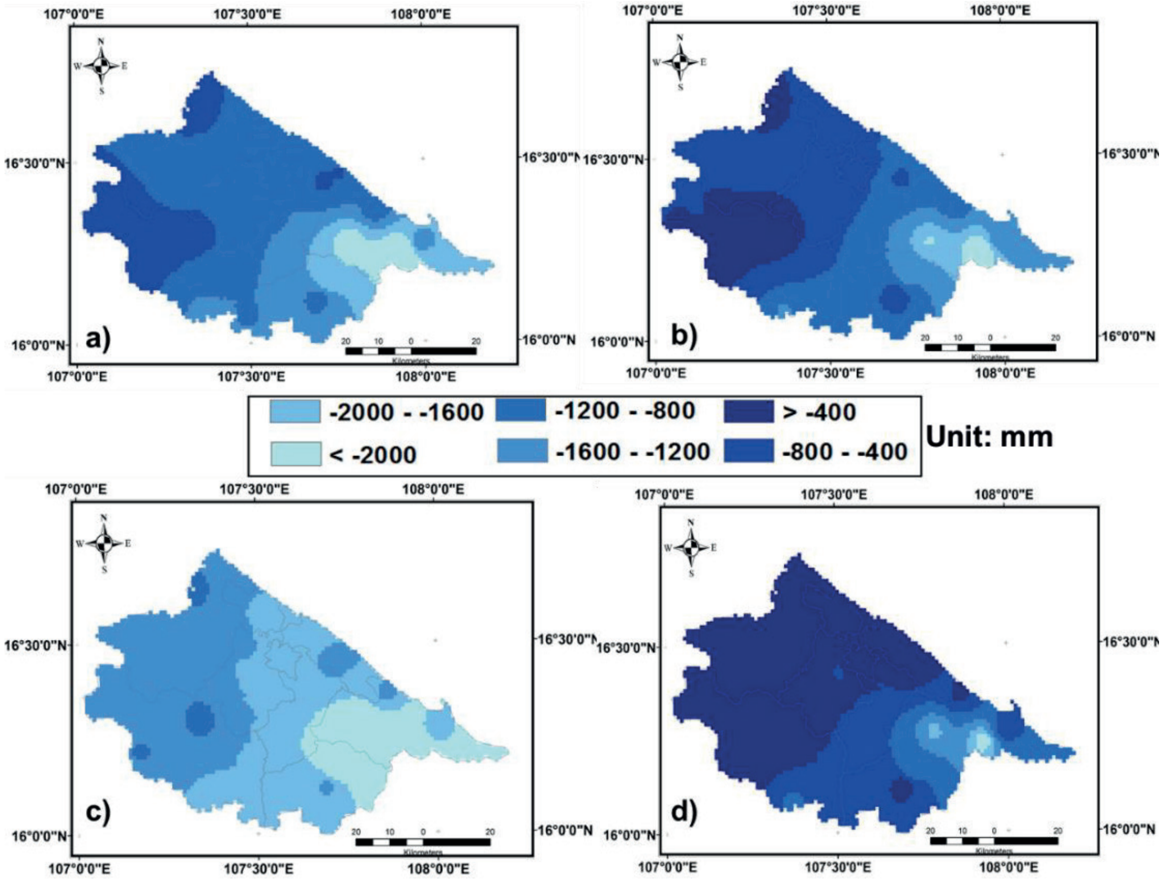

Fig. 7. Spatial distribution of precipitation datasets against observation for MSWEP (a), CHIRPS (b), GPM (c) and GSMAP (d) during Sep–Nov of 2021

observed precipitation, capturing the spatial variability well. However, slight underestimations persist in some regions, particularly in the central and southern parts. Generally, in 2021, MSWEP continues to provide the most balanced and accurate representation of rainfall. GSMaP overestimates, whereas CHIRPS and GPM struggle with underestimation, particularly in extreme rainfall zones.

For 2022, MSWEP remains the most balanced and accurate dataset. GSMaP tends to overestimate, whereas CHIRPS and GPM struggle with underestimation, particularly for extreme events.

In this study, the comparative evaluation of four satellite-based precipitation datasets comprising CHIRPS, GSMaP, GPM and MSWEP is also implemented for different subregions based on the three key statistical metrics of RMSE, MAE and R. The regions are analyzed based on topography in which region1 refers to the western mountains, region2 refers to coastal plains and region3 refers to the southern mountains.

As seen in Figure 10, among the datasets, MSWEP stands out as the most accurate, exhibiting the lowest RMSE and MAE, coupled with the highest correlation coefficient (R=0.58). This indicates that MSWEP provides the best agreement with observed precipitation data, particularly in capturing temporal and spatial variations. In contrast, CHIRPS and GSMaP show the poorest performance, with both datasets displaying the highest RMSE (>50 mm/day) and substantial MAE, suggesting a tendency to overestimate or underestimate precipitation. While GPM outperforms CHIRPS and GSMaP in terms of RMSE and MAE, its relatively low correlation (R=0.34) suggests limited reliability in capturing precipitation variability. Overall, MSWEP emerges as the most reliable dataset for precipitation estimation, making it a preferable choice for hydrological modeling and climate studies for the western mountains (Fig. 10).

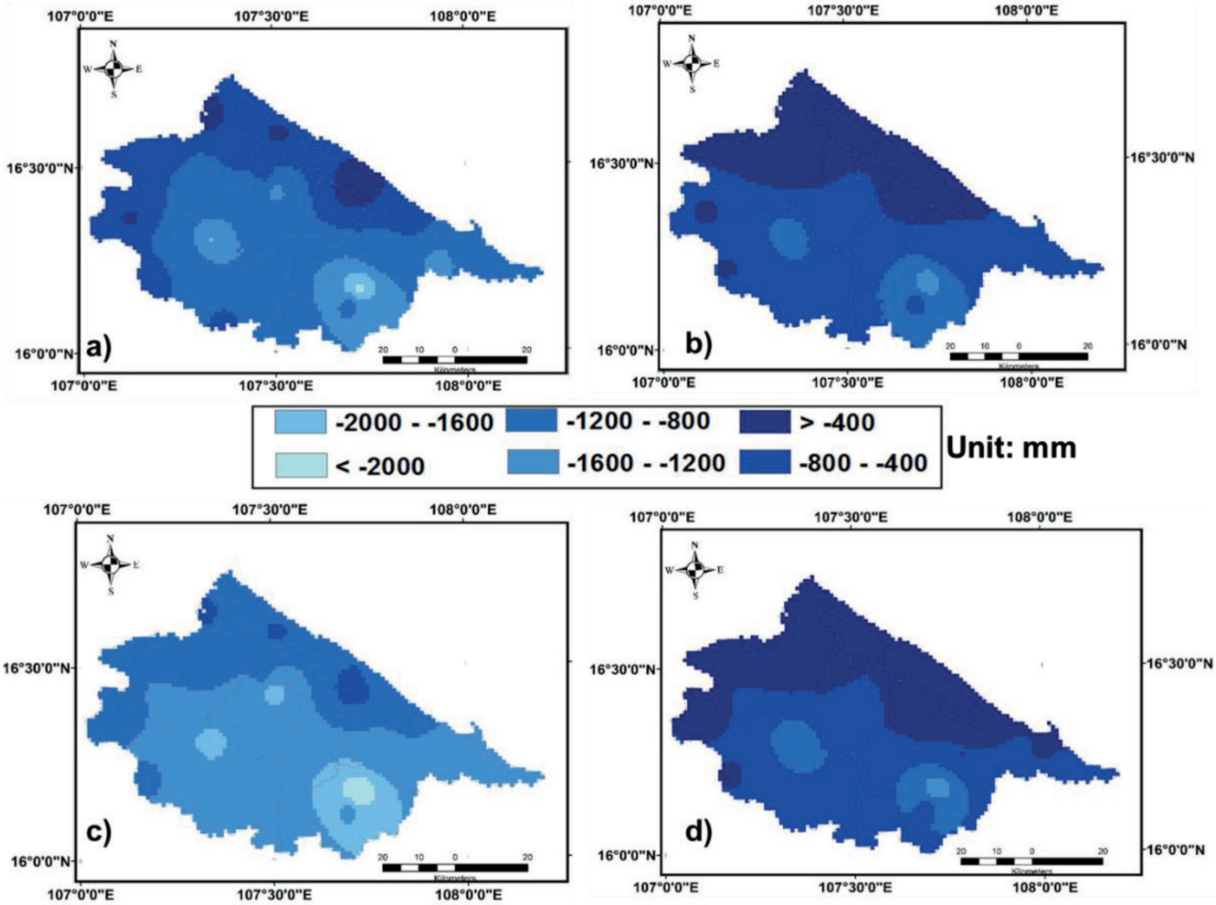

Fig. 8. Spatial distribution of precipitation datasets against observation for MSWEP (a), CHIRPS (b), GPM (c) and GSMAP (d) during Sep–Nov of 2022

Meanwhile, for the coastal plains, GSMaP exhibits the highest correlation (R=0.63) but also has a relatively high RMSE, indicating improved temporal alignment but persistent biases. MSWEP performs well overall, with high correlation (R=0.58) and lower RMSE, making it a reliable dataset. CHIRPS and GPM show weaker correlations (R=0.39 and 0.34, respectively) and high RMSE values, indicating limitations in accuracy. GSMaP's strong correlation suggests better event detection, but MSWEP balances accuracy and consistency, making it the most reliable choice for precipitation analysis (Fig. 11).

For the southern mountains, the comparison of CHIRPS, GSMaP, GPM and MSWEP highlights notable differences in precipitation performance. MSWEP shows the highest correlation (R=0.51) and balanced error metrics, making it the most reliable dataset. GSMaP follows with R=0.33 but exhibits a high RMSE, indicating systematic biases. CHIRPS and GPM have the weakest correlations (R=0.33 and 0.31, respectively), suggesting poor agreement with observations. Overall, MSWEP stands out as the best-performing dataset, while GSMaP shows moderate accuracy, and CHIRPS and GPM require caution in applications due to lower reliability.

Thua Thien Hue is strongly controlled by individual, or combinations of, basic synoptic patterns such as storms or tropical depressions, intertropical convergence zone, cold air. Nguyen and Bui (2003) showed four weather patterns causing heavy rainfall from (1) low troughs or cyclones combined with strong easterly winds, (2) storms or tropical depressions landfall or effect in combination with intertropical convergence zone, (3) individual storms or tropical depression landfall or effect, and (4) cold air combined with intertropical convergence zone. Data from more than 30 years ago shows that cold air combined with storms or tropical depressions was the primary cause of floods,

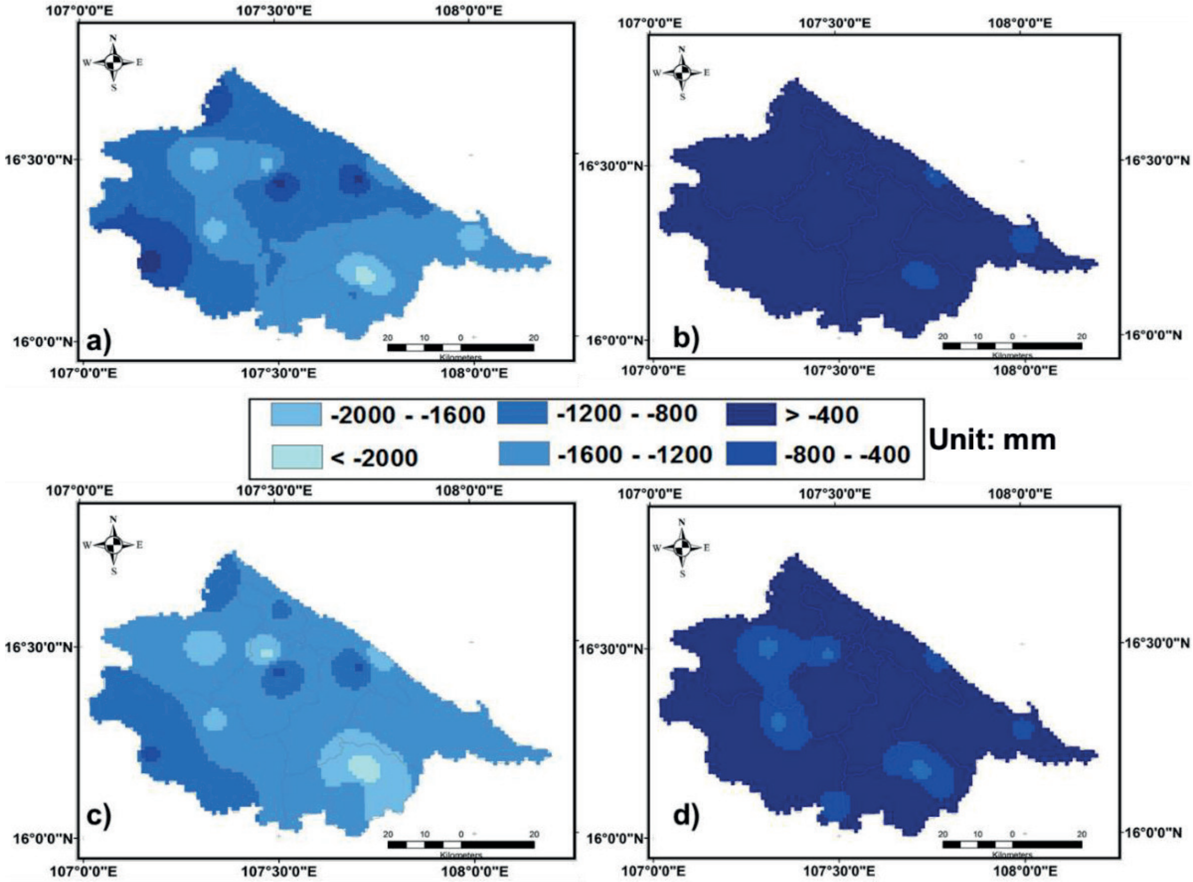

Fig. 9. Spatial distribution of precipitation datasets against observation for MSWEP (a), CHIRPS (b), GPM (c) and GSMAP (d) during Sep–Nov of 2023

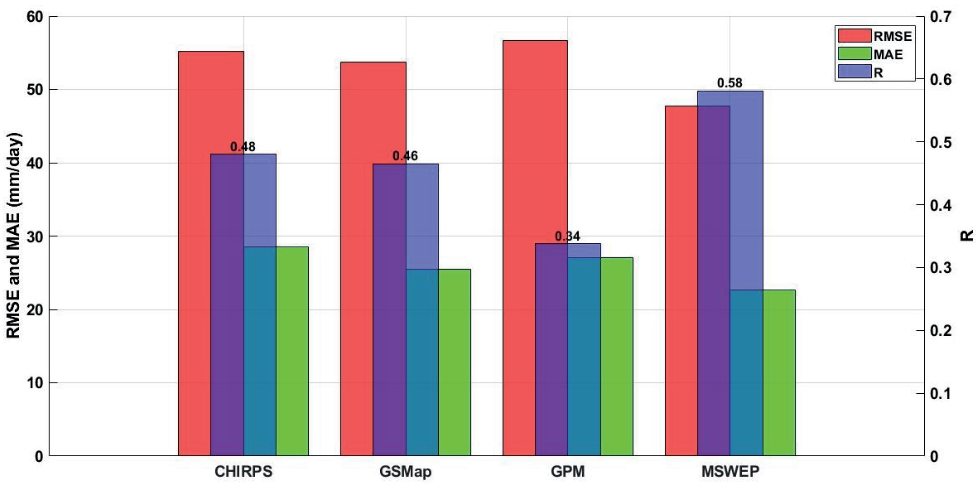

Fig. 10. Statistical metrics of temporal performance for region1

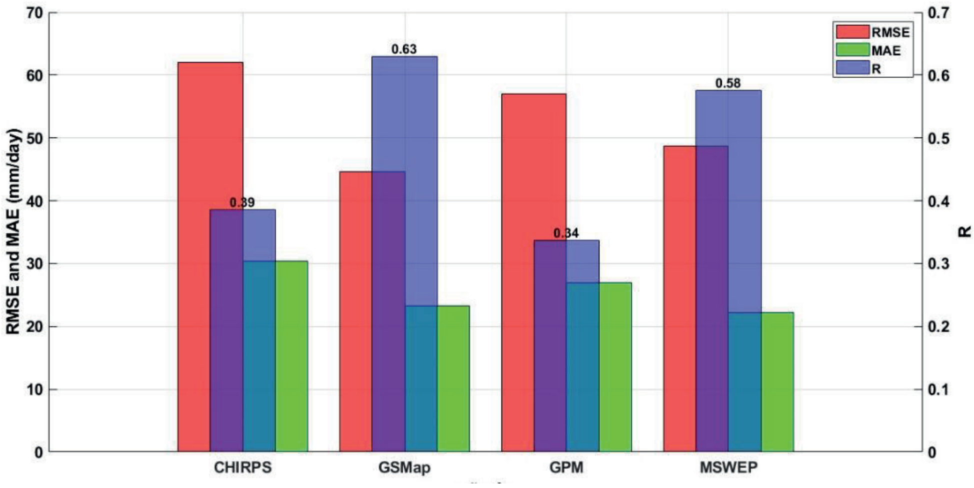

Fig. 11. Statistical metrics of temporal performance for region2

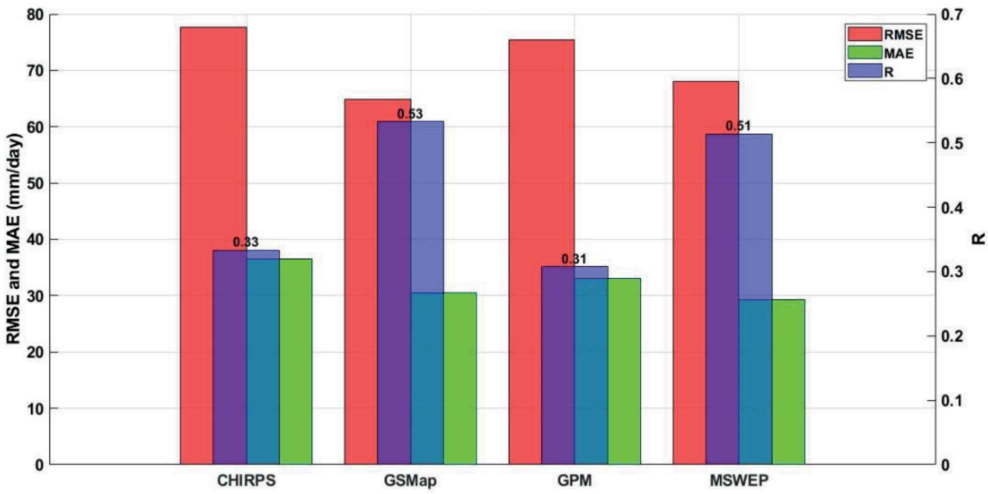

Fig. 12. Statistical metrics of temporal performance for region3

accounting for 20.7% of occurrences. This was followed by storm or tropical depression formation at 18.6%, and cold air combined with strong easterly winds at 14.5%. This partly contributes to the uncertainty of satellite-based precipitation products. Importantly, the effect of Bach Ma Mountain as a barrier, forcing moist air from the sea, combined with the Truong Son mountains located in the west of the province, very likely causes heavy rainfall and rainfall patterns that are temporally and spatially even. The heavy rainfall could come from the combination of rugged terrain and granite geology. This relates to the locality and complicated nature of rainfall variations and significantly contributes to the uncertainty of precipitation products for Thua Thien Hue.

Event-based evaluation

The 3D scatter plot visualizes the relationship between observed precipitation, GSMaP and MSWEP. The color gradient represents OBS values, with darker shades (purple) indicating lower rainfall and lighter shades (yellow) indicating higher rainfall.

The results showed dense clustering in the lower range, with most data points being concentrated in the low precipitation range (0–20 mm) for all three

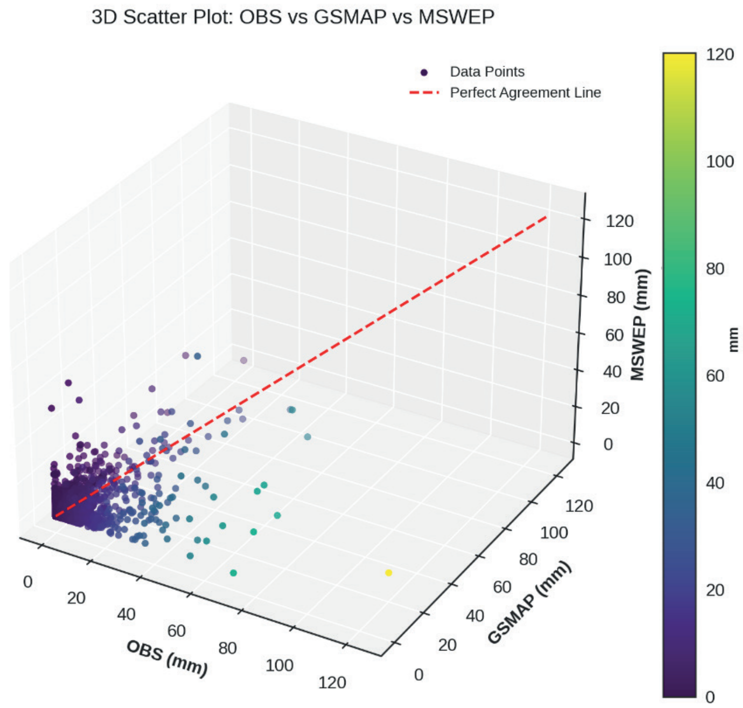

Fig. 13. 3D scatter plot of OBS, GSMAP and MSWEP

datasets, indicating an underestimation tendency of extreme rainfall events for both GSMaP and MSWEP. At higher observed rainfall values, GSMaP exhibits higher variability compared to MSWEP, which remains relatively lower. This suggests that GSMaP could capture more extreme rainfall values than MSWEP, though possibly with overestimation. The spread along the MSWEP axis is more limited compared to GSMaP, implying that MSWEP generally underestimates rainfall events compared to OBS. Generally, the scattered distribution suggests that neither GSMaP nor MSWEP perfectly aligns with OBS values, highlighting potential biases and uncertainties in satellite-based precipitation estimates. More importantly, GSMaP appears to capture higher rainfall values but with greater variability, whereas MSWEP tends to underestimate precipitation more consistently. Both datasets show limitations in extreme event estimation (Fig. 13).

Furthermore, according to the World Meteorological Organization, the rain intensity classifications within three hours are light rainfall (0–2.5 mm), moderate rainfall (2.6–7.5 mm), heavy rainfall (7.6–15 mm), very heavy rainfall (15.1–30 mm) and extreme rainfall (greater than 30 mm). Based on that, as seen in Fig. 14, all three datasets (i.e., OBS, GSMAP, MSWEP) show the highest frequency in the "light rainfall" category (above 90%). This indicates that most satellite- and gauge-based rainfall events are of low intensity. Importantly, GSMAP has a slightly lower frequency of light rainfall compared to OBS but higher than MSWEP. The frequency of higher rainfall categories including moderate, heavy, very heavy and extreme varies slightly. In general, the GSMAP and MSWEP datasets exhibit minor discrepancies compared to OBS but still capture the overall rainfall distribution. These data can be valuable for climate research and weather forecasting, but further validation is necessary to assess the accuracy of each dataset.

Obviously, the findings from the event-based evaluation of precipitation products are very important to models of hydrological processes that are importantly related to flood peaks and that often use sub-daily rainfall series as input. Long-term series of sub-daily precipitation data are necessary to provide valuable insights into extreme weather events and to then identify the periods of flood for potential assessment in precipitation patterns. Over this study, however, sub-daily precipitation data have only been available since 2020; this is a limitation of the study.

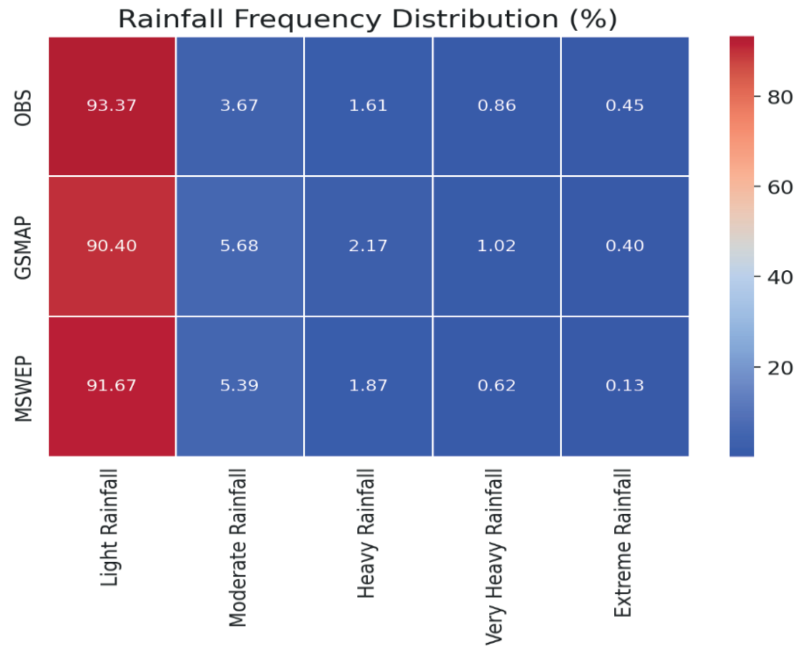

Fig. 14. Rainfall frequency distribution (%)

Conclusion and recommendations

This study evaluated CHIRPS, GSMaP, GPM and MSWEP against ground observations in Thua Thien Hue (2020–2023) across both temporal and spatial scales. The results are based on cumulative rainfall, Taylor diagram, spatial Distribution and Bias Analysis, statistic metrics of temporal performance for regions, and particularly event-based evaluation. Accordingly, the results highlight that MSWEP aligns well with observations in the western mountains and coastal plains, whereas GSMaP captures variability in the southern mountains. CHIRPS and GPM exhibit larger biases, particularly in extreme rainfall zones. All datasets could capture rainfall events but need refinement for extreme precipitation. For the extreme and very extreme precipitation records in Thua Thien Hue, GSMaP is the best of the products analyzed. In general, the findings show that MSWEP is the most reliable dataset and should be considered, followed by GSMaP, for hydrological applications. CHIRPS and GPM showed a weaker agreement, tending to underestimate rainfall. The authors suggest that further investigations should focus on improving the accuracy of satellite-based rainfall products (e.g., CHIRPS and GPM) in the region through bias-correction techniques combined with deep learning and climatic parameters on a regional scale.

Disclosure statement

No potential conflict of interest was reported by the authors.

Author contributions

Study design: NTS, NTT; data collection: NTS, NTT; statistical analysis: NTS, NTT; result interpretation: NTS, NTT; manuscript preparation: NTT; literature review: NTS, NTT.

References

ASHOURI H, HSU K-L, SOROOSHIAN S, BRAITHWAITE DK, KNAPP KR, CECIL LD, NELSON BR, PRAT OP, 2015, PERSIANN-CDR: Daily Precipitation Climate Data Record from Multisatellite Observations for Hydrological and Climate Studies. *Bulletin of the American Meteorological Society* 96: 69–8. DOI: https://doi.org/10.1175/BAMS-D-13-00068.1.

BECK HE, WOOD EF, PAN M, FISHER CK, MIRALLES DM, VAN DIJK AIJM, MCVICAR TR and ADLER

RF, 2019, MSWEP V2 global 3-hourly 0.1° precipitation: methodology and quantitative assessment. *Bulletin of the American Meteorological Society* 100(3): 473–500. DOI: https://doi.org/10.1175/BAMS-D-17-0138.1.

BURTON C, SAMI R and YADVINDER M, 2018, Inter-comparison and assessment of gridded climate products over tropical forests during the 2015/2016 El Niño. *Philosophical Transactions of the Royal Society B: Biological Sciences* 373(1760): 20170406. DOI: 10.1098/rstb.2017.0406.

FUNK C, PETERSON P, LANDSFELD M, PEDREROS D, VERDIN J, SHUKLA S, HUSAK G, ROWLAND J, HARRISON L, HOELL A and MICHAELSEN J, 2015, The Climate Hazards Infrared Precipitation with Stations—A New Environmental Record for Monitoring Extremes. *Science Data* 2: 150066. DOI: https://doi.org/10.1038/sdata.2015.66.

HAI BT, TUAN NV, 2018, Research on the Assessment and Comparison of High-Resolution Rainfall Data in the Ca River Basin. *Journal of Meteorology and Hydrology* 2018: 17-28.

JI H, DINGZHI P, YU G, YAQI L, and XIAOYU L, 2022, Evaluation of multiple satellite precipitation products and their potential utilities in the Yarlung Zangbo River Basin. *Scientific Reports* 12(1): 13334. DOI: https://doi.org/10.1038/s41598-022-17551-y.

KIDD C and HUFFMAN G, 2011, Global precipitation measurement. *Meteorological Applications* 18(3): 334-353. DOI: https://doi.org/10.1002/met.284.

LUO H, ZHIQIANG L, HAIMENG C, DIXIANG X, GONG C and DONGSHENG S, 2024, Assessments of multiple precipitation products and application in hydrodynamic simulations: A case of casualty-inducing mountain torrents in Sichuan, Southwest China. *Journal of Flood Risk Management* 17(4): e13016. DOI: https://doi.org/10.1111/jfr3.13016.

LYU Y, BIN Y, FAN H, WEIQING Q, FUQIANG T, GUOQING W and JIANYUN Z, 2024, Investigating twelve mainstream global precipitation datasets: Which one performs better on the Tibetan Plateau? *Journal of Hydrology* 633: 130947. DOI: https://doi.org/10.1016/j.jhydrol.2024.130947.

MONRE, 2023, Disaster risk zones, maps for warning of tropical cyclones, storms and storm-driven water surge (in Vietnamese).

NGUYEN KV and BUI MT, 2003, The characteristics of weather synoptic situations causing very heavy rains, serious inundation, and floods in Quang Binh, Quang Tri, Thua Thien Hue provinces (in Vietnamese). *Journal of Earth sciences* 25(4): 339-345. DOI: https://doi.org/10.15625/0866-7187/25/4/11432.

PANG Z, YU Z, CHUNXIANG S, JUNXIA G, QINGJUN Y, YANG P, ZHENG W and BIN X, 2023, A comprehensive assessment of multiple high-resolution precipitation grid products for monitoring heavy rainfall during the 7.20 extreme rainstorm event in China. *Remote Sensing* 15(21): 5255. DOI: https://doi.org/10.3390/rs15215255.

People's Committee of Thua Thien Hue Province (PCTTHP), Committee, 2005, Geography of Thua Thien Hue - Natural Part. Social Sciences Publishing House, Hanoi (In Vietnamese).

People's Committee of Thua Thien Hue Province (PCTTHP), Committee, 2020, Summary report of natural disaster prevention (In Vietnamese).

PRESS WH, TEUKOLSKY SA, VETTERING WT and FLANNERY BP, 2003, Numerical recipes in c++: The art of scientific computing (2nd ed.) 1 numerical recipes example book (c++)(2nd ed.) 2 numerical recipes multi-language code cd rom with linux or unix single-screen license revised version3. *European Journal of Physics* 24(3): 329-330. DOI: 10.1088/0143-0807/24/3/701.

SAIKRANTHI K, RAO TN, RAJEEVAN M and BHASKARA RAO SV, 2013, Identification and validation of homogeneous rainfall zones in India using correlation analysis. *Journal of Hydrometeorology* 14(1): 304-317. DOI: https://doi.org/10.1175/JHM-D-12-071.1.

SIMPSON J, ADLER RF and NORTH GR, 1988, A proposed tropical rainfall measuring mission (TRMM) satellite. *Bulletin of the American meteorological Society* 69(3): 278-295. DOI: https://doi.org/10.1175/1520-0477(1988)069<0278:APTRMM>2.0.CO;2.

THANH NT, 2019, Evaluation of multi-precipitation products for multi-time scales and spatial distribution during 2007-2015. *Civil Engineering Journal* 5(1): 255-267. DOI: 10.28991/cej-2019-03091242.

USHIO T, KUBOTA T, SHIGE S, OKAMOTO K, AONASHI K, INOUE T, TAKAHASHI N, IGUCHI T, KACHI M, OKI R, MORIMOTO T and KAWASAKI Z, 2009, A Kalman filter approach to the Global Satellite Mapping of Precipitation (GSMaP) from combined passive microwave and infrared radiometric data. *Journal of the Meteorological Society of Japan* 87A: 137–151. DOI: https://doi.org/10.2151/jmsj.87A.137.

ZHOU Z, GUO B, XING W, ZHOU J, XU F and XU Y, 2020, Comprehensive evaluation of latest GPM era IMERG and GSMaP precipitation products over mainland China. *Atmospheric Research Journal* 246: 105132. DOI: https://doi.org/10.1016/j.atmosres.2020.105132.

Received 24 October 2024
Accepted 13 May 2025